

Ehrenfest Dynamics and Frictionless Cooling Methods

Stephen Choi,¹ Roberto Onofrio,^{2,3} and Bala Sundaram¹

¹*Department of Physics, University of Massachusetts, Boston, MA 02125, USA*

²*Dipartimento di Fisica e Astronomia “Galileo Galilei”, Università di Padova, Via Marzolo 8, Padova 35131, Italy*

³*ITAMP, Harvard-Smithsonian Center for Astrophysics, 60 Garden Street, Cambridge, MA 02138, USA*

Recently introduced methods which result in shortcuts to adiabaticity, particularly in the context of frictionless cooling, are rederived and discussed in the framework of an approach based on Ehrenfest dynamics. This construction provides physical insights into the emergence of the Ermakov equation, the choice of its boundary conditions, and the use of minimum uncertainty states as indicators of the efficiency of the procedure. Additionally, it facilitates the extension of frictionless cooling to more general situations of physical relevance, such as optical dipole trapping schemes. In this context, we discuss frictionless cooling in the short-time limit, a complementary case to the one considered in the literature, making explicit the limitations intrinsic to the technique when the full three-dimensional case is analyzed.

PACS numbers: 37.10.-x, 03.65.Sq

I. INTRODUCTION

Cooling quantum systems to the lowest reachable temperatures is a goal with motivations arising both from fundamental and practical considerations. The ultimate control of microscopic systems in the ultracold regime allows for the full exploitation of quantum technologies as well as the understanding of the attainability of zero temperature. Much of the focus in cooling has been on the manipulation of populations in energy levels, through coupling to external reservoirs, with the goal of increasing occupancy of the lowest energy levels. However, an alternative strategy consists of temporally manipulating a parameter of the system Hamiltonian to reduce the energy content of each level while keeping occupancy invariant. These strategies are “adiabatic” in the fullest sense, both thermodynamic and quantum, as they neither change the entropy nor the energy distribution of the system.

Usual adiabatic protocols require changing a Hamiltonian parameter such that the rate of change of the parameter times its duration is much smaller than its absolute initial value. This requirement severely constrains the cooling power, making adiabatic cooling techniques less favorable in those contexts where, in addition to the intrinsic dynamics, sources of decoherence and noise exist, hindering desired tasks such as quantum computation or simulation. Techniques to achieve shortcuts to adiabaticity relax this condition by only requiring constancy of entropy at the initial and final times, but not necessarily at intermediate times. By identifying a global time invariant, temporal trajectories of the Hamiltonian parameter can be found such that the final population distribution equals the initial one while all the energy eigenvalues are scaled down by a common factor. This cooling technique, known as “frictionless cooling,” sketched in the conclusions of Ref. [1], has been extended to an atomic framework [2] leading to an increasing number of applications [3, 4]. Adiabatic or frictionless cooling does not reduce the entropy of the system under consideration [5],

making it ineffective for situations in which entropy and phase space density play the leading role such as in triggering phase transitions. However, these techniques do reduce the temperature, with all the associated benefits in terms of state preparation [6]. Examples include efficient fast decompression of ^{87}Rb atoms in normal [7] and Bose-condensed [8] states, which have been experimentally demonstrated, and detailed proposals for efficient fast atomic transport [9] and optimized sympathetic cooling [10].

In harmonic potentials, frictionless cooling is achieved by choosing the variability of the trap frequency as specified by the solution of a second order differential equation, the Ermakov equation. In our earlier work [11], we had addressed the robustness of this protocol to realistic sources of uncertainties and errors, and had shown that the Ermakov solution leads to minimum uncertainty wavepackets at both initial and final times. Additionally, this protocol resulted in squeezing of the momentum variance, formally parametrized through Bogoliubov transformations, during the dynamical evolution. This allowed us to use the degree of squeezing seen in the evolved solution as an effective measure of fidelity. However, the reasons behind the emergence of minimum uncertainty states at the final time, and not during intermediate times, were not made explicit. In this paper, we fill in some of these gaps in understanding this technique by considering the Ehrenfest dynamics of the Heisenberg operator equations for the time-dependent harmonic oscillator [12, 13]. In particular, the physical interpretation of variables in the Ermakov construction, the choice of boundary conditions, and the role of squeezing in the solution all become manifest. We also extend the construction to a special case where the dynamics is restricted to the class of generalized Gaussian states, which results in the so-called Effective Gaussian Dynamics (EGD) approach [14, 15]. While both Ehrenfest dynamics and EGD approach are exact for quadratic potentials, more generally they are known to provide approximate but valid results specifically at short times [16], which makes

them well-suited for application to frictionless cooling methods in their fastest regime.

The paper is organized as follows. In Section II we provide a brief introduction to the general Heisenberg operator approach and the special EGD case. In Section III this formalism is applied to the important case of harmonic oscillator or quadratic potential and provide a brief discussion of the resulting set of equations. In Section IV we explicitly show the connection of our construction to frictionless cooling in the case of harmonic potentials. In Section V we discuss possible extensions within the EGD framework, with particular emphasis on the experimentally relevant case of optical dipole trapping. Finally we conclude with some qualitative insights on the usefulness of Heisenberg operator equations to further expand the concept of frictionless cooling.

II. HEISENBERG OPERATOR EQUATIONS AND EHRENFEST DYNAMICS

We begin our analysis considering a general time-dependent Hamiltonian $\hat{H} = \hat{p}^2/2m + V(\hat{x}, t)$. The associated Heisenberg equations are:

$$\begin{aligned}\frac{d\hat{x}}{dt} &= \frac{\hat{p}}{m}, \\ \frac{d\hat{p}}{dt} &= -\frac{\partial V(\hat{x}, t)}{\partial \hat{x}}.\end{aligned}\quad (1)$$

Writing each operator $\hat{A} = \langle \hat{A} \rangle + \Delta \hat{A}$, where $\langle \dots \rangle$ denotes the expectation value so that $\langle \Delta \hat{A} \rangle = 0$, one can Taylor expand the potential $V(\hat{x}, t)$ about $\langle \hat{x} \rangle$ resulting in the following pair of Ehrenfest equations

$$\frac{d\langle \hat{x} \rangle}{dt} = \frac{\langle \hat{p} \rangle}{m}, \quad (2)$$

$$\frac{d\langle \hat{p} \rangle}{dt} = -\sum_{n=0}^{\infty} \frac{1}{n!} V^{(n+1)}(\langle \hat{x} \rangle) \langle \Delta \hat{x}^n \rangle, \quad (3)$$

where $V^{(n)} = \partial^n V / \partial x^n$. Writing down the corresponding evolution equations for $\langle \Delta \hat{x}^n \rangle$ leads to an infinite hierarchy of equations. It is worth noting here that the functional form of $V(\hat{x}, t)$ is important in coupling higher moments to the evolution of the centroid variables. The infinite set of moment equations are typically truncated using one of a number of possible approximations, largely determined by the nature of the problem being addressed [17].

Of course, one can truncate the infinite equations order by order which is equivalent to approximating any potential as a polynomial, where the degree is related to the order of the correlations that are retained. However, this truncation leads to the coupling of moments across different orders as soon as one goes beyond the second order. This results in higher-order moments becoming dynamically significant even if they were initially (at $t = 0$) zero. The only exception to this behavior is

the special case of a quadratic potential where, at each order, the moment equations depend only on other moments of the same order. This is readily illustrated by writing down the second-order contributions

$$\frac{d\langle \Delta \hat{x}^2 \rangle}{dt} = \frac{1}{m} \langle \Delta \hat{x} \Delta \hat{p} + \Delta \hat{p} \Delta \hat{x} \rangle, \quad (4)$$

$$\frac{d\langle \Delta \hat{x} \Delta \hat{p} + \Delta \hat{p} \Delta \hat{x} \rangle}{dt} = \frac{2}{m} \langle \Delta \hat{p}^2 \rangle - 2V^{(2)}(\langle \hat{x} \rangle) \langle \Delta \hat{x}^2 \rangle, \quad (5)$$

$$\frac{d\langle \Delta \hat{p}^2 \rangle}{dt} = -V^{(2)}(\langle \hat{x} \rangle) \langle \Delta \hat{x} \Delta \hat{p} + \Delta \hat{p} \Delta \hat{x} \rangle \quad (6)$$

The more general result for the evolution equations for higher-order moments can be readily written down, although with tedium increasing progressively with each order.

It is clear that straight truncation up to second order may not be effective for arbitrary, non-quadratic potentials. Improved accuracy in arbitrary potentials while keeping the number of Ehrenfest equations finite is desirable. In this regard, another related method to truncate the infinite hierarchy of moment equations involves the use of a time-dependent variational approach in which the state of the system is assumed to remain in a general Gaussian form. The major implication of the Gaussian approximation is that higher-order correlations can be expressed in terms of one and two-point correlations alone, leading to a dramatic truncation in the space of variables. Also, given that arbitrary operators A , B , and C with $[A, B] = iC$ implies [18]

$$\langle A^2 \rangle \langle B^2 \rangle \geq \frac{1}{4} \langle C \rangle^2 + \frac{1}{4} \langle AB + BA \rangle^2, \quad (7)$$

the general Gaussian form obeys the uncertainty relation

$$\langle \Delta \hat{x}^2 \rangle \langle \Delta \hat{p}^2 \rangle = \frac{\hbar^2}{4} + \frac{1}{4} \langle \Delta \hat{x} \Delta \hat{p} + \Delta \hat{p} \Delta \hat{x} \rangle^2, \quad (8)$$

which helps to simplify the Ehrenfest equations. The resulting EGD is represented by [14, 15]

$$\frac{dx}{dt} = \frac{p}{m}, \quad (9)$$

$$\frac{dp}{dt} = -\sum_{n=0}^{\infty} V^{(2n+1)}(x) \frac{\rho^{2n}}{n! 2^n}, \quad (10)$$

$$\frac{d\rho}{dt} = \frac{\Pi}{m}, \quad (11)$$

$$\frac{d\Pi}{dt} = \frac{\hbar^2}{4m\rho^3} - \sum_{n=0}^{\infty} V^{(2n+2)}(x) \frac{\rho^{2n+1}}{n! 2^n}, \quad (12)$$

where $x \equiv \langle \hat{x} \rangle$ and $p \equiv \langle \hat{p} \rangle$ are the expectation values of position and momentum, respectively. Here, odd cumulants are identically zero and even cumulants can be written in terms of variable ρ as $\langle \Delta \hat{x}^{2n} \rangle = \rho^{2n} 2n! / (2^n n!)$. We also introduce a new variable $\Pi = \langle \Delta \hat{x} \Delta \hat{p} + \Delta \hat{p} \Delta \hat{x} \rangle / 2\rho$ which, as is clear from its definition, reflects the correlation between $\Delta \hat{x}$ and $\Delta \hat{p}$. Together, the four equations of

motion fully describe the evolution of both the centroid and the spreading of the wave packet.

Before considering the case of the time-dependent harmonic oscillator which serves as a useful paradigm for frictionless cooling methods, an important difference between EGD and the second-order truncation methods is worth noting. The second-order truncation consists of locally approximating an arbitrary potential by an effective quadratic one and, in keeping with the Heisenberg picture, places no restrictions on the wavefunction. By contrast, the EGD method assumes a Gaussian state which in terms of the potential results in a polynomial approximation involving only even powers. Thus, in the general case, these two approximations are different and are valid for differing evolution times. As we see in the next section, an exception is the case of a harmonic potential where the two methods converge.

III. EHRENFEST DYNAMICS FOR A HARMONIC OSCILLATOR

Given our motivation of connecting the Ehrenfest equations to those seen in frictionless cooling methods, we specifically consider the case of a harmonic trap with a time-dependent angular frequency, *i.e.* $V(x, t) = \frac{1}{2}m\omega^2(t)x^2$. In this instance, both the more general approach Eqs. (2)-(6) and the EGD yield identical and considerably simplified relations

$$\frac{dx}{dt} = \frac{p}{m}, \quad (13)$$

$$\frac{dp}{dt} = -m\omega^2(t)x, \quad (14)$$

$$\frac{d\rho}{dt} = \frac{\Pi}{m}, \quad (15)$$

$$\frac{d\Pi}{dt} = \frac{\hbar^2}{4m\rho^3} - m\omega^2(t)\rho. \quad (16)$$

It is clear that in this specific case of the harmonic oscillator, Eqs. (13) and (14), and Eqs. (15) and (16) are completely decoupled, and one can look at the evolution of the mean position and momentum completely independently of the evolution of the respective fluctuations, allowing for an easy numerical integration. Also, it is interesting that, due to the structure of the equations, Eq. (16) can describe the case of an external potential that includes up to a linear term in position via an arbitrary, in general time-dependent, constant $\beta(t)$, *i.e.* $V(x, t) = \frac{1}{2}m\omega^2(t)x^2 + \beta(t)x$.

The decoupling of the centroid and fluctuation relations allows the recasting of the problem in terms of a higher-dimensional system where the fluctuation and average variables are treated on an equal footing. In terms of the canonical variable pairs (x, p) and (ρ, Π) , the extended Hamiltonian $H_{ext} \equiv \langle H \rangle$ is given by $H_{ext} =$

$H_{px} + H_{\Pi\rho}$ where

$$H_{px} = \frac{p^2}{2m} + \frac{1}{2}m\omega^2(t)x^2, \quad (17)$$

$$H_{\Pi\rho} = \frac{\Pi^2}{2m} + \frac{\hbar^2}{8m\rho^2} + \frac{1}{2}m\omega^2(t)\rho^2. \quad (18)$$

A number of remarks are now in order. First, the extended Hamiltonian has a centrifugal barrier which prevents $\rho \rightarrow 0$ except in the trivial, classical limit in which we can assume $\hbar \rightarrow 0$. Second, the quantum correction preventing null position fluctuations is proportional to the second power of the Planck constant, consistently with the osmotic term present in the Madelung-Bohm form of the Schrödinger equation [19]. Third, it is simple to show that the effective potential for the fluctuating part – if expanded around the minimum for an oscillator with constant frequency – generates small fluctuations with average value oscillating harmonically in time (‘breathing’ modes) with frequency twice the oscillator frequency. This fact is exploited in stroboscopic quantum nondemolition measurements of position [20, 21]. Finally, the decoupling of the first and second moments is a particular case, for a single particle, of Kohn’s theorem valid in the more general situation of an interacting many-body system [22].

IV. CONNECTION TO FRICTIONLESS COOLING

The goal of this Section is to derive from the Ehrenfest perspective the results of frictionless cooling as described in [2]. In order to make this contribution self-consistent, we briefly recall that the Ermakov trajectory, prescribing the time variation of the harmonic trapping frequency necessary for frictionless cooling, arises from the Lewis-Riesenfeld invariant $I(t) = 1/2[\pi^2/m + m\omega_0^2(q/b)^2]$, where $\pi = bp - m\dot{b}q$. The invariant is obtained, as first shown by Ermakov [23], by introducing an auxiliary equation to the Newtonian equation for the harmonic oscillator, which determines the evolution of a scaling factor b related to the position variable $x = q/b$. The resulting Ermakov equation is given by

$$\ddot{b} + \omega^2(t)b = \omega_0^2/b^3. \quad (19)$$

In order for the invariant $I(t)$ to commute with the Hamiltonian (given as Eq. (3) in [2]) it is necessary that at $t = 0$, $b(0) = 1$ and $\dot{b}(0) = 0$. Also the choice $\ddot{b}(0) = 0$ ensures that $\omega(0) = \omega_0$. At $t = t_f$ the conditions $b(t_f) = (\omega_0/\omega_f)^{1/2}$, $\dot{b}(t_f) = 0$, and $\ddot{b}(t_f) = 0$ are imposed. These make sure that $I(t)$ commutes with the Hamiltonian at $t = t_f$ and that $\omega(t_f) = \omega_f$. These six boundary conditions suggests a fifth-order polynomial Ansatz for $b(t)$, facilitating a solution of the Ermakov equation for $b(t)$, and subsequently the explicit Ermakov trajectory for the angular frequency $\omega(t)$.

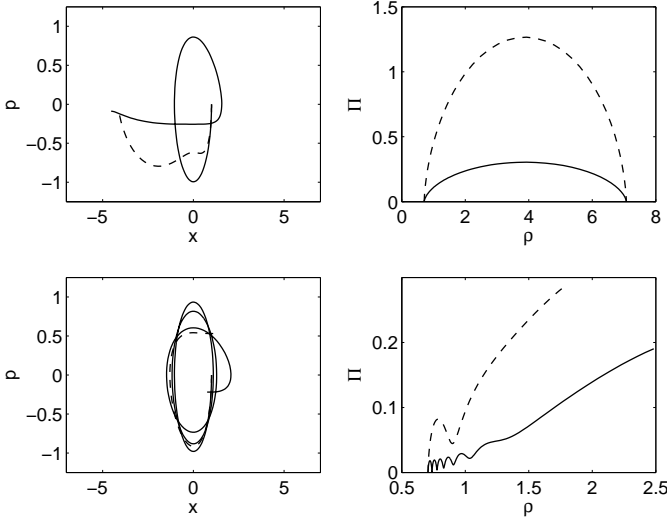


FIG. 1: Generalized phase space plots of the Ehrenfest dynamics in the case of the harmonic oscillator. Here and in all the subsequent figures, all variables are given in harmonic oscillator units, with $\hbar = m = 1$. By definition Π has units of harmonic oscillator momentum. In the top row we depict the case of a harmonic oscillator driven through a Ermakov trajectory, with the solid line corresponding to $t_f = 25$ ms, and the dashed line to a faster frictionless cooling occurring in $t_f = 6$ ms (see also Fig. 4 in [28]). On the left we report the centroid dynamics, p vs. x , on the right column the fluctuation dynamics, Π vs. ρ . For comparison, in the bottom row we report the same quantities for the case of a linear ramping-down of the frequency occurring in the same time durations, showing that in the 25 ms case the harmonic oscillator performs several cycles with respect to the corresponding Ermakov trajectory. Notice that the Ermakov trajectories in the fluctuational phase space always lead to a final minimum uncertainty state $\Pi = 0$, unlike the linear ramp-down trajectories.

The scaling factor $b(t)$ is proportional to the standard deviation of the wave function $\sigma(t)$, such that for the ground state $n = 0$, $b(t) = \sigma(t)/(\hbar/2m\omega_0)^{1/2}$, i.e. the standard deviation expressed in harmonic oscillator length units, $a_0 = (\hbar/2m\omega_0)^{1/2}$ [2]. This allows us to make the identification with the parameter ρ in Eqs. (15-16) $a_0 b(t) \equiv \rho(t) \equiv \sigma(t)$. In particular, one can condense the four equations Eqs. (13-14), and Eqs. (15-16) into two second-order differential equations

$$\frac{d^2 x}{dt^2} = -\omega^2(t)x, \quad (20)$$

$$\frac{d^2 \rho}{dt^2} = \frac{\hbar^2}{4m^2 \rho^3} - \omega^2(t)\rho, \quad (21)$$

where, again, Eq. (20) is completely decoupled from Eq. (21). The first is nothing but the Newton equation for the harmonic oscillator while the equation for the spreading of the wave packet, Eq. (21), can be rearranged as

$$\ddot{\rho} + \omega^2(t)\rho = (\hbar^2/4m^2)/\rho^3, \quad (22)$$

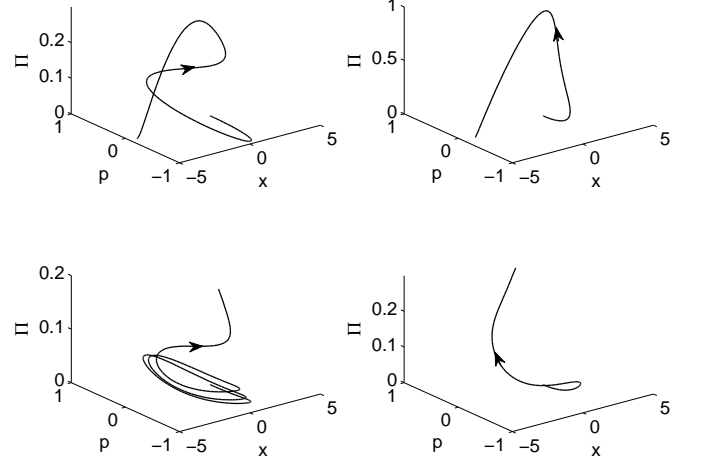


FIG. 2: Plot of Π vs. p and x for the cases shown in Fig. 1. The left column corresponds to $t_f = 25$ ms, the right column to $t_f = 6$ ms, the top row is for the Ermakov trajectory, the bottom row for the corresponding linear ramping with the same t_f . An increasing Π as seen in the linear ramping cases leads to larger squeezing of the final wavefunction and an increasing departure from the desired minimum uncertainty state.

which coincides with the Ermakov equation by identifying $\omega_0^2 = \hbar^2/(4m^2 a_0^4)$ along with $b = \rho/a_0$. Therefore the Ermakov equation obtained through a proper, but less physically insightful, identification of an invariant naturally emerges here from the Ehrenfest formulation[24]. The identification of b with ρ also means that is not possible to impose Dirichlet boundary conditions, since ρ cannot be zero. Solving the equations under Neumann boundary conditions makes clear the underpinning for the minimum uncertainty state seen at $t = t_f$.

Additionally, one can identify $ma_0 \dot{b}(t) = \Pi(t)$. The boundary conditions imposed $\dot{b}(0) = \dot{b}(t_f) = 0$ translate into $\Pi(0) = \Pi(t_f) = 0$. In our earlier work [11], we found that the Ermakov trajectory requires a minimum uncertainty wavepacket at both initial and final times $t = 0$ and $t = t_f$ which, in the terminology of the moments, equates to $\Pi = 0$ at these times. So when we follow the Ermakov trajectory $\omega(t)$ it is now not surprising that a minimum uncertainty state is achieved at $t = t_f$, as this is *enforced* by the *unique* choice of boundary conditions. Notice also that the momentum variance, related to the temperature of the ultracold gas, can be written in terms of ρ and Π as $\langle \Delta \hat{p}^2 \rangle = \hbar^2/(4\rho^2) + \Pi^2$, from the uncertainty relation Eq. (8), which shows that momentum fluctuations are reduced if ρ is made large and, simultaneously, $\Pi = 0$. This relationship makes it clear that a mere increase of the position variance ρ (e.g. by directly relaxing the trap frequency) with the goal of reducing the corresponding momentum variance does not necessarily work unless the system reaches a minimum uncertainty

state at the final time. Removal of squeezing correlations through $\Pi = 0$ is therefore the key step in a frictionless cooling scheme.

Furthermore, the boundary conditions $\ddot{b}(0) = \ddot{b}(t_f) = 0$ imply $\dot{\Pi}(0) = \dot{\Pi}(t_f) = 0$, and Eq. (21) then gives the width ρ consistent with the eigenstate of a harmonic trap with the correct angular frequencies at $t = 0$ and $t = t_f$, as it should. It is worth noting that in the true adiabatic limit one starts with a minimum uncertainty wavepacket (associated with the initial frequency $\omega(0)$) and it remains a minimum uncertainty packet for all times during the evolution. This requires $\Pi = 0$ and $d\Pi/dt = 0$ for all t . Any deviation from this leads to diabatic transitions which can be countered by non-zero values of Π . It is interesting that this is precisely the counter-diabatic anticommutator term found in other approaches to achieve shortcuts to adiabaticity [25–27].

We have explicitly confirmed the validity of the Ehrenfest dynamics and EGD for the time-dependent quadratic potential by using the numerically obtained Ermakov trajectory as the input for $\omega(t)$ in Eqs (13 - 16). The time evolution of the variables was found to be identical to those obtained by numerically integrating the full Schrödinger Equation. This agreement holds even for trajectories involving short t_f which includes an antitrapping stage. The Gaussian Ansatz of EGD implies that the wave function remains a coherent state even in the presence of an inverted trap as the time is too short for the wave function to start breaking up.

The phase space diagrams for x vs. p and ρ vs. Π are shown in Fig. 1 for different cooling protocols. As in our previous work [10, 11], we consider two representative final times in all of our simulations – $t_f = 25$ ms and $t_f = 6$ ms – where the 6 ms case involves an anti-trapping stage while the 25 ms case does not. We compare the Ermakov trajectory (top row) to the case of a quasi-adiabatic protocol obtained with a linear ramp of the frequency in the same time interval (bottom row). As expected, the Ermakov trajectory gives $\Pi = 0$ at the end of the run, implying that the state returns to the minimum uncertainty state as a consequence of the imposed boundary conditions, while the linear ramp case shows non-zero final Π . A three-dimensional plot is presented in Fig. 2 to show more explicitly the evolution of squeezing along the trajectories. A more direct representation of this dynamics in terms of the corresponding Wigner function has been discussed in Ref. [29].

V. EXTENSIONS TO OPTICAL DIPOLE TRAPPING USING GAUSSIAN BEAMS

Fast expansion methods have also been discussed in the more realistic case of optical Gaussian-beam traps in Ref. [30]. This is a more intriguing case than usual magnetic traps since, unlike the latter, trapping frequencies along the radial and axial direction (in the almost universally adopted confinement geometry with radial symme-

try) cannot be independently controlled. Nevertheless, optical dipole traps enjoy several advantages in ultra-cold atom experiments, among these the possibility to trap spinor condensates, the flexibility in independently using magnetic fields (for instance to exploit magnetic Feshbach resonances), the possibility to trap atoms with no permanent magnetic moment, and the possibility for atomic control with higher spatial and temporal resolution. It is therefore worthwhile to discuss to what extent frictionless cooling techniques may be applied to this important class of trapping schemes. We will deal with the simplest situation of a single Gaussian beam of wavelength λ red-detuned with respect to the dominant atomic transition λ_{at} . Taking into account the intensity profile of a Gaussian laser beam in the paraxial approximation, and identifying a symmetry axis in the direction of the light propagation along the z axis, the effective potential energy felt by the atoms is given, in terms of the radial and axial coordinates r and z , as

$$V_{\text{opt}}(r, z, t) = V_0(t) \left[1 - \frac{w_0^2}{w^2(z)} e^{-2r^2/w^2(z)} \right], \quad (23)$$

where $V_0(t) = 3I_0(t)\lambda^3/(16\pi^2 c \tau \delta)$, with $I_0(t)$ the instantaneous beam intensity, τ the lifetime of the excited state, $\delta = \lambda - \lambda_{\text{at}}$ the detuning between the light wavelength and the atomic transition wavelength, w_0 the beam waist, and $w(z) = w_0 \sqrt{1 + (z/z_R)^2}$ the spot size at location z , where $z_R = \pi w_0^2/\lambda$ is the Rayleigh range.

On applying the EGD to this effectively 2D situation, one gets two sets of equations Eqs. (9 - 12) for the radial and axial directions. In each direction, the expectation values and two-point correlations decouple and each gives rise to its own Ermakov-type fluctuation equations. Explicit EGD equations are given by evaluating Eqs. (10) and (12) using the Gaussian optical potential of Eq. (23) for the experimentally reasonable case of $\langle r \rangle = \langle z \rangle = 0$. From now on, we shall use the simplified notation $r \equiv \langle r \rangle$ and $z \equiv \langle z \rangle$.

In the radial direction, the infinite series can be evaluated using the properties of Hermite polynomials to give $V_{\text{opt}}^{(2n+1)}(r) = 0$ for all n . By using various identities involving the generalized Laguerre polynomials the series that includes the partial derivatives $V_{\text{opt}}^{(2n+2)}(r)$ can, after some work, be evaluated to finally yield

$$\frac{d^2 r}{dt^2} = 0, \quad (24)$$

$$\frac{d^2 \rho_r}{dt^2} = \frac{\hbar^2}{4m^2 \rho_r^3} - \frac{4V_0(t)}{mw_0^2} \rho_r \left[1 + \left(\frac{2\rho_r}{w_0} \right)^2 \right]^{-3/2}. \quad (25)$$

In the axial direction, we have instead a Lorentzian function in z as our $V_{\text{opt}}(r, z, t)$ and it turns out that, again, $V_{\text{opt}}^{(2n+1)}(z) = 0$ for all n , while the partial derivatives

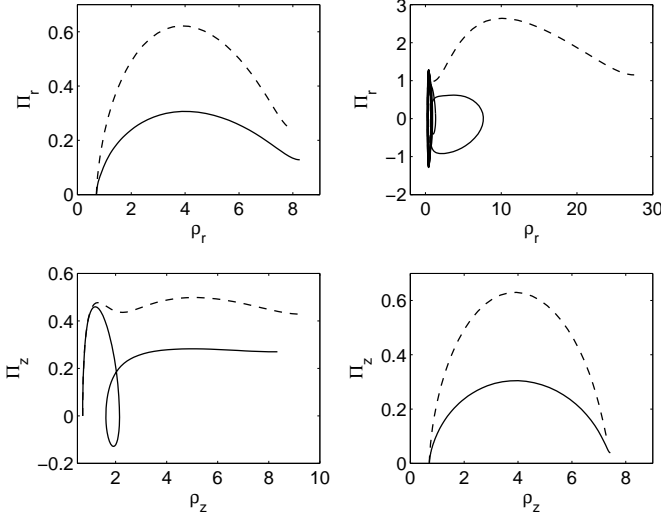


FIG. 3: Ehrenfest dynamics for the optical dipole potential as in Eq. (23) expressed through the fluctuative components in the Π vs. ρ phase diagram. The top row represents the radial variables Π_r and ρ_r , the bottom row is for the axial variables Π_z and ρ_z . In the left column the Ermakov driving $\omega_r^2(t)$ is imposed on the radial frequency, in the right column the axial frequency is instead Ermakov-driven with $\omega_z^2(t)$. We have chosen a beam waist of $w_0 = 20a_0$, and as usual we consider two different times $t_f = 25$ ms (solid line) and $t_f = 6$ ms (dashed line).

$V_{opt}^{(2n+2)}(z)$ are found to simplify to give

$$\frac{d^2 z}{dt^2} = 0, \quad (26)$$

$$\frac{d^2 \rho_z}{dt^2} = \frac{\hbar^2}{4m^2 \rho_z^3} - \frac{V_0(t)}{m z_R^2} \rho_z \sum_{n=0}^{\infty} \frac{(2n+2)!}{n!} \left(-\frac{\rho_z^2}{2z_R^2} \right)^n \quad (27)$$

The Newtonian relations (24) and (26) make it clear that the expansion is around the equilibrium point $r = z = 0$. The corresponding extended Hamiltonians in the Π - ρ space are given by

$$H_{\Pi_r \rho_r} = \frac{\Pi_r^2}{2m} + \frac{\hbar^2}{8m \rho_r^2} - V_0(t) \left[1 + \left(\frac{2\rho_r}{w_0} \right)^2 \right]^{-1/2} \quad (28)$$

$$H_{\Pi_z \rho_z} = \frac{\Pi_z^2}{2m} + \frac{\hbar^2}{8m \rho_z^2} + \frac{V_0(t)}{z_R^2} \sum_{n=0}^{\infty} \frac{(2n+1)!}{n!} \times \left(-\frac{1}{2z_R^2} \right)^n \rho_z^{2n+2}. \quad (29)$$

In the limit of small ρ_r and ρ_z (or large w_0 and z_R) one can approximate Eqs. (25) and (27) to rederive the Ermakov equations

$$\frac{d^2 \rho_r}{dt^2} = \frac{\hbar^2}{4m^2 \rho_r^3} - \frac{4V_0(t)}{m w_0^2} \rho_r, \quad (30)$$

$$\frac{d^2 \rho_z}{dt^2} = \frac{\hbar^2}{4m^2 \rho_z^3} - \frac{2V_0(t)}{m z_R^2} \rho_z. \quad (31)$$

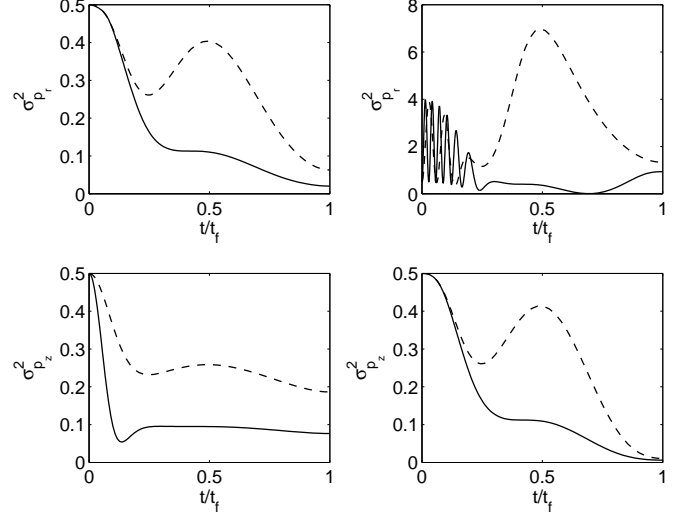


FIG. 4: Time evolution of the momentum variance for the same arrangement as in Fig. 3

Comparing with the general form for the Ermakov Equation, we get the equivalent Ermakov angular frequencies $\omega_r^2(t) = 4V_0(t)/m w_0^2$ and $\omega_z^2(t) = 2V_0(t)/m z_R^2$. These are exactly the forms obtained by Muga and collaborators [30] and despite the decoupling of the radial and axial coordinates, $\omega_r^2(t)$ and $\omega_z^2(t)$ are related through $V_0(t)$

$$\omega_z^2(t) = \frac{w_0^2}{2z_R^2} \omega_r^2(t). \quad (32)$$

This implies that optimal fast-adiabatic cooling can only be achieved in either one of the radial and axial directions for a given run *i.e.* the other direction may not be simultaneously cooled optimally, hopefully undergoing a sort of indirect, passive frictionless cooling.

We numerically simulate the full EGD relations, Eqs. (25) and (27), and consider two cases, which are motivated by the relationship between axial and radial trap frequencies. The first is the *master radial* case when $\omega_r^2(t)$ is set to be the Ermakov trajectory (and hence $\omega_z^2(t)$ follows a modified trajectory as given in Eq. (32)), and the second is the *master axial* case for the inverse situation. For illustrative purposes, we shall consider here the less ideal case of small w_0 and z_R , *i.e.* away from the Ermakov limits of Eqs. (30) and (31) in our numerical simulations. We shall take the minimum Rayleigh length that permits paraxial approximation, $z_R = 2w_0$ (typically z_R is much larger, for example $z_R = 24w_0$ in [30]). Also we choose the small beam waist of $w_0 = 20$ and 200 harmonic oscillator lengths, based on the fact that the size of a typical beam waist can range from $w_0 = 8 \mu\text{m}$ (as in [30] which is of the order 53 harmonic oscillator lengths for ^{87}Rb atoms) to sizes of order 0.3 mm (corresponding to roughly 2,000 harmonic oscillator lengths).

Figure 3 shows the Π vs. ρ phase diagram, where the top row presents the phase space diagram for the radial variables Π_r and ρ_r and the bottom row is for the axial

w_0	t_f (ms)	Master Radial				Master Axial			
		$\langle \Delta \hat{p}_r^2 \rangle$	Π_r	$\langle \Delta \hat{p}_z^2 \rangle$	Π_z	$\langle \Delta \hat{p}_r^2 \rangle$	Π_r	$\langle \Delta \hat{p}_z^2 \rangle$	Π_z
20	25	0.0202	0.1285	0.0764	0.2699	0.9337	-0.4687	0.0060	0.0386
20	6	0.0627	0.2425	0.1864	0.4283	1.3265	1.1516	0.0104	0.0759
200	25	0.0050	0.0017	0.0769	0.2711	1.0618	1.0268	0.0050	0.0004
200	6	0.0050	0.0035	0.1733	0.4128	34.5122	5.8745	0.0050	0.0009

TABLE I: Final radial and axial $\langle \Delta \hat{p}^2 \rangle$ and Π for the *master radial* and *master axial* cases. All variables are given in harmonic oscillator units, with $\hbar = m = 1$. In particular, the beam waist w_0 is expressed in units of the harmonic oscillator length $a_0 = (\hbar/2m\omega_0)^{1/2}$ which, with $\omega_0/2\pi = 250$ Hz, corresponds to $a_0 = 0.95 \mu\text{m}$ and $0.49 \mu\text{m}$ in the most representative examples of ^{23}Na and ^{87}Rb atoms, respectively.

variables Π_z and ρ_z . In the left column the *master radial* case is depicted, while the right column is describing the *master axial* case. Fig. 4 has the same arrangement as Fig. 3 except that the momentum variance time evolution is presented. The results shown in Figs. 3 and 4 are obtained for a beam waist $w_0 = 20a_0$. A tenfold increase in the beam waist results in the same qualitative behavior and the corresponding values for $\langle \Delta \hat{p}^2 \rangle$ and Π are presented in Table I.

From the results we can see better *master axial* performance both in terms of the reduction in the momentum variance and the restoration of the minimum uncertainty state indicated by Π approaching zero. The results are practically indistinguishable from simulating the Ermakov limit, Eq. (31). This is to be expected, since, even with the deliberately less ideal choice of $w_0 = 20a_0$ and $z_R = 2w_0$, the magnitudes of the coefficient of ρ_z^{2n} in the series of Eq. (27) quickly drops to zero for increasing n . For instance, up to $n = 5$ the magnitudes are: 2 , 7.5×10^{-3} , 3.52×10^{-5} , 2.05×10^{-7} , 1.44×10^{-9} . On the other hand, for efficient cooling in both directions, the *master radial* case with $t_f = 25$ ms works better since the performance in the axial direction is not as severely compromised as in the inverse case. In general the $t_f = 25$ ms cases yields better results in terms of cooling, being closer to $\Pi = 0$.

We notice that in the top right hand panel of Fig. 3 (Π_r vs. ρ_r for the *master axial* arrangement) the phase space trajectory for $t_f = 6$ ms covers a relatively large area compared to the corresponding counterpart in the bottom left panel (Π_z vs. ρ_z for the *master radial* arrangement). This can be understood from the difference in the extended Hamiltonians Eq. (28) and (29). If plotted, the potential for the axial Hamiltonian overlaps very closely to the case of a quadratic potential, while the potential for the radial Hamiltonian deviates from the quadratic case as ρ_r becomes larger, such that the potential decreases with a greater (negative) slope compared to the quadratic case. This makes it easier for the ρ_r variable to extend to a greater distance from the origin, especially with an antitrapping stage included in the $t_f = 6$ ms case.

Another observation is the attainment of negative Π in Fig. 3 for $t_f = 25$ ms in the “subordinate” cases (axial under *master radial* situation and vice versa). One can understand the negative Π from the extended Hamilto-

nian as a function of Π and ρ , where, in the Π direction the function is simply parabolic and not multiplied by the Ermakov trajectory $\omega(t)$. Initially $\Pi = 0$ then it grows over time due to squeezing $\Pi > 0$, *i.e.* rolls “up-hill” and then it turns around to roll back down. For the longer non-optimal time of $t_f = 25$ ms, it seems reasonable that there is enough time to roll up to the other side of the hill attaining $\Pi < 0$. Physically, from the evolution equations, negative Π is seen to result in a decrease in the corresponding ρ variable. This means a reduction in the spatial width or the “contractive” behavior associated with the so-called twisted coherent states introduced in [31] (see also [32] for the contractive behavior of Schrödinger cat states). The negative values of Π do not impact the uncertainty relation since the latter depends on Π^2 .

VI. CONCLUSIONS

We have discussed frictionless cooling in terms of the Ehrenfest dynamics, getting more physical insight into the detailed nature of the cooling process, and analyzed the relevant example of an optical dipole trap in the short-time duration regime which is complementary to the analysis reported in [30]. This approach is also a simpler alternative to the search for Ermakov invariants in higher dimensional spaces as discussed in [33] since in our framework the time-dependent frequencies are related to second derivatives of the potential evaluated at the expectation values.

The fact that the Ermakov equation emerges for the case of a harmonic potential via the application of EGD in which a Gaussian wave packet Ansatz is imposed throughout the evolution is consistent with the concept of adiabatic following, where an energy eigenstate remains so throughout the evolution. One may therefore view the EGD as generating a subspace of solutions that “simulate” the behavior of adiabatic following. Alternatively, it can be viewed as a way to naturally include the counter-diabatic term in the Hamiltonian [25–27]. Formally, one should be able to generalize this idea to any arbitrary eigenstates and trapping potentials. As mentioned above, the Gaussian wave packet in a quadratic potential is the only case that involves a small number of

tractable, closed set of equations as an infinite chain of equations involving all cumulants results in other situations (for instance see [34] for the application to a double-well system). However, it is reassuring that higher order cumulants do not play a significant role for short times, and therefore should not make invalid the dynamics in situations in which a very short duration of the protocol is chosen. In this sense, and noting that solutions which are less than absolutely optimal may be sufficient for some cooling situations, we suggest that this “Ansatz-enforced” shortcut to adiabaticity may be applicable in more general situations. The procedure would start by truncating the Taylor expansion around the centroid in the Ehrenfest equations to N terms, with the truncation being exact for potentials described by an N th order polynomial. This would result in a finite number of moment equations to be satisfied, instead of a single

Ermakov Equation as in the case of a Gaussian Ansatz in a harmonic potential. One can proceed by solving iteratively a truncated set of cumulant equations with an appropriate Ansatz imposed, using progressively more equations for higher accuracy. The high order moments could additionally be controlled by the imposition of appropriate boundary conditions.

Finally, it is noted that having $\omega(0) \ll \omega(t_f)$ one should also obtain a “fast-adiabatic heating” effect, and this observation is more transparent in the Ehrenfest framework as this corresponds to generalized phase space trajectories for the cumulants related to fast-adiabatic cooling via time-reversal. The added ability to deal with more general potentials and targeted final thermal states may be relevant to recent research activity in the context of quantum engines [35–37].

-
- [1] C. Yuce, A. Kilic, and A. Coruh, *Phys. Scr.* **74**, 114 (2006).
 - [2] X. Chen, A. Ruschhaupt, S. Schmidt, A. del Campo, D. Guéry-Odelin, and J. G. Muga, *Phys. Rev. Lett.* **104**, 063002 (2010).
 - [3] J.-F. Schaff, P. Capuzzi, G. Labeyrie, and P. Vignolo, *New J. Phys.* **13**, 113017 (2011).
 - [4] E. Torrontegui, S. Ibáñez, S. Martínez-Garaot, M. Modugno, A. del Campo, D. Guéry-Odelin, A. Ruschhaupt, X. Chen, and J. G. Muga *Adv. At. Mol. Opt. Phys.* **62**, 117 (2013).
 - [5] W. Ketterle and D. E. Pritchard, *Phys. Rev. A* **46**, 4051 (1992).
 - [6] We also mention here an alternative way to speed up the time evolution of a quantum system, named “fast-forward of adiabatic dynamics”, see S. Masuda and K. Nakamura, *Phys. Rev. A* **78**, 062108 (2008); *Proc. R. Soc. A* **466**, 1135 (2010). Although similar in spirit to frictionless cooling, this technique differs from the latter as it relies on the application of driving potentials depending on the initial state, and does not deal explicitly with thermal states.
 - [7] J.-F. Schaff, X.-L. Song, P. Vignolo, and G. Labeyrie, *Phys. Rev. A* **82**, 033430 (2010).
 - [8] J.-F. Schaff, X.-L. Song, P. Capuzzi, P. Vignolo, and G. Labeyrie, *EPL* **93**, 23001 (2011).
 - [9] E. Torrontegui, S. Ibáñez, X. Chen, A. Ruschhaupt, D. Guéry-Odelin, and J. G. Muga, *Phys. Rev. A* **83**, 013415 (2011).
 - [10] S. Choi, R. Onofrio, and B. Sundaram, *Phys. Rev. A* **84**, 051601(R) (2011).
 - [11] S. Choi, R. Onofrio, and B. Sundaram, *Phys. Rev. A* **86**, 043436 (2012).
 - [12] P. Ehrenfest, *Zeit. f. Physik* **45**, 455 (1927).
 - [13] The term “Ehrenfest dynamics”, though not commonly used among physicists, is quite established in other contexts. See, for instance, X. Li, J. C. Tully, H. B. Schlegel, and M. J. Frisch, *J. Chem. Phys.* **123**, 084106 (2005).
 - [14] A. K. Pattanayak and W. C. Schieve, *Phys. Rev. A* **46**, 1821 (1992).
 - [15] A. K. Pattanayak and W. C. Schieve, *Phys. Rev. E* **50**, 3601 (1994).
 - [16] See, for example, B. Sundaram and P. W. Milonni, *Phys. Rev. E* **51**, 1971 (1995), and references therein.
 - [17] Examples of this point can be found in P. Hänggi and P. Talkner, *J. Stat. Phys.* **22**, 65 (1980) and L. E. Ballentine and S.M. McRae, *Phys. Rev. A* **58**, 1799 (1998).
 - [18] H. P. Robertson, *Phys. Rev.* **34**, 163 (1929); E. Schrödinger, *Sitz. Preuss. Akad. Wissen.* **14**, 296 (1930); J. L. Powell and B. Crasemann, *Quantum Mechanics*, Addison-Wesley (Reading MA, 1963).
 - [19] E. Madelung, *Zeit. f. Physik* **40**, 322 (1926).
 - [20] V. B. Braginsky, I. Vorontsov, and F. Ya. Khalili, *Sov. Phys. JETP Lett.* **27**, 276 (1978). [*Pis'ma Zh. Eksp. Teor. Fiz.* **27**, 296 (1978)].
 - [21] K. S. Thorne, R. W. P. Drever, C. M. Caves, M. Zimmerman, and V. D. Sandberg, *Phys. Rev. Lett.* **40**, 667 (1978).
 - [22] W. Kohn, *Phys. Rev.* **123**, 1242 (1961).
 - [23] V. P. Ermakov, *Univ. Izv. Kiev* **20**, 1 (1880).
 - [24] We note that the same relationship can be found in constructing a new class of coherent states. A. K. Rajagopal, and J. T. Marshall, *Phys. Rev. A* **26**, 2977 (1982).
 - [25] M. Demiralp and S. A. Rice, *J. Chem. Phys.* **129**, 154111 (2008).
 - [26] C. Jarzynski, *Phys. Rev. A* **88**, 040101(R) (2013).
 - [27] A. del Campo, *Phys. Rev. Lett.* **111**, 100502 (2013).
 - [28] S. Ibáñez, S. Martínez-Garaot, X. Chen, E. Torrontegui, and J. G. Muga, *Phys. Rev. A* **84**, 023415 (2011).
 - [29] D. Schuch, *Phys. Lett. A* **338**, 225 (2005).
 - [30] E. Torrontegui, X. Chen, M. Modugno, A. Ruschhaupt, D. Guéry-Odelin, and J. G. Muga, *Phys. Rev. A* **85**, 033605 (2012).
 - [31] H. P. Yuen, *Phys. Rev. Lett.* **51**, 719 (1983).
 - [32] L. Viola and R. Onofrio, *New J. Phys.* **5**, 1 (2003).
 - [33] P. G. L. Leach, *Phys. Lett. A* **158**, 102 (1991).
 - [34] H. Hasegawa, *arXiv:1301.6423v3* (2013).
 - [35] Y. Rezek and R. Kosloff, *New J. Phys.* **8**, 83 (2006).
 - [36] O. Abah *et al.*, *Phys. Rev. Lett.* **109**, 203006 (2012).
 - [37] J. Deng *et al.*, *arXiv:1307.4182* (2013).